DC-DC Converter for PV Module Integration

Estefanía Ruiz, Aitor Teran, Nicolai Fransen, Jesper Kloster, Thassilo Lang, Nicolás Murguizur Bustos

Energy Technology, INTRO-760, 2018-12

Master's Project

Here you can write something about which tools and software you have used for typesetting the document, running simulations and creating figures. If you do not know what to write, either leave this page blank or have a look at the colophon in some of your books.

Electronics and IT
Aalborg University
http://www.aau.dk

AALBORG UNIVERSITY
STUDENT REPORT

Title:
DC-DC Converter for PV Module Integration

Theme:
Scientific Theme

Project Period:
Fall Semester 2018

Project Group:
INTRO-760

Participant(s):
Estefanía Ruiz, Aitor Teran
Nicolai Fransen, Jesper Kloster
Nicolás Murguizur Bustos
Thassilo Lang

Supervisor(s):
Lajos Török
Dezso Sera

Copies: 1

Page Numbers: 40

Date of Completion:
November 16, 2018

Abstract:

Here is the abstract

Contents

Todo list

Preface

Here is the preface. You should put your signatures at the end of the preface.

Aalborg University, November 16, 2018

Estefanía Ruiz
eruiza18@student.aau.dk

Aitor Teran
ateran18@student.aau.dk

Nicolai Fransen
nfrans18@student.aau.dk

Jesper Kloster
jklost18@student.aau.dk

Thassilo Lang
tlang18@student.aau.dk

Nicolás Murguizur Bustos
nmurgu18@student.aau.dk

Nomenclature

Abreviations:

AC	Alternating Current
DC	Direct Current
FET	Field-Effect Transistor
IC	Integrated Circuit
MIC	Module Integrated Converter
MOSFET	Metal Oxide Semiconductor Field-Effect Transistor
MPP	Maximum Power Point
MPPT	Maximum Power Point Tracking
PBL	Problem Based Learning
PV	Photovoltaic
PWM	Pulse Width Modulation
SEPIC	Single Ended Primary Inductance Converter
STC	Standard Test Conditions

Symbols:

η	Efficiency
°C	Degree Celsius
D	Duty Cycle
E	Energy
I	Current
I_{mpp}	MPP Current
I_{sc}	Short Circuit Current
N	Number of PV Panels
P	Power
P_{max}	Maximum Power
t	Time
V	Voltage
V_{ds}	Drain Source Voltage
V_{mpp}	MPP Voltage
V_{oc}	Open Circuit Voltage
W	Watt
W/m^2	Irradiance

1 Introduction

To this date, sustainable energy sources have become an area of worldwide focus in an attempt to reduce the environmental impact due to emissions of CO_2 and other greenhouse gasses. The development of competitive systems to exploit renewable energy sources is the best alternative to reduce the use of fossil fuels for the production of electricity. Over the last years, there has been a considerable increase in electricity production from renewable energy sources being the fastest growing sectors wind and solar energy. In 2017, photovoltaic generation was the renewable energy source which experienced the highest increase in newly installed capacity. The total installed capacity reached approximately 402 GW[1].

Photovoltaic (PV) is referred to the production of electricity in the form of direct current (DC) directly from sunlight shining on solar cells. Solar cells are semiconductor devices which typically can produce around 0.5 V DC so they are series connected to form a PV panel which can also be connected to other PV panels resulting in a PV array [2]. This way, according to the system's requirements, the PV panels can be interconnected in series or parallel in order to get at the output a higher voltage or current, respectively. Connecting PV panels either in series or parallel will result in an increase of the system's overall electricity production.

Nevertheless, it is essential to keep into consideration the mismatches that may appear on the power generated by the different PV panels. This will result in losses in the PV system and thus in a lower efficiency. Mismatches may lead to uneven power generation. These can be caused to partial shading, manufacturing tolerances, defects in the PV modules due to weather conditions and ageing among others. Even a small mismatch in one of the PV modules can result in a very high reduction of the power production from the entire PV array [3]. Mismatch losses in a PV system can be reduced by forcing every PV module to work at its Maximum Power Point (MPP) by using a technique known as Maximum Power Point Tracking (MPPT). This can be reached by using electronic devices called Module Integrated

Converters (MICs). MICs consist on DC-AC micro inverters or DC-DC converters that incorporate a MPPT controller unit to ensure that the output power of the MIC is the one corresponding to the MPP of the PV module [3].

1.1 Photovoltaic generation

The generation of direct current electricity from solar energy is a phenomenom known as *Photovoltaic effect* which was first discovered by a French physicist named Edmond Becquerel in 1839 [4]. This process allows the generation of electrical energy in a solar cell, which is composed of two layers of semiconductor material (usually silicon), when it is exposed to the sunlight [4]. The greater the intensity of the light (irradiance) that is absorbed by the PV panel, the higher the amount of electric power generated. On the other hand, the efficiency of the panel decreases with increasing temperature [2]. Usually, PV panels are tested under standard test conditions (STC) to indicate the performance of the PV modules. The STC test is carried out at a solar cell's temperature of 25°C and at a solar irradiance of 1000 W/m^2 [2]. When the temperature of the PV cell is higher than 25°C, the PV panel generates less power and at a lower temperature the electricity generation is improved [2].

Some of the most important characteristics associated with a PV panel's datasheet are the following: maximum power (P_{max}), open-circuit voltage (V_{oc}), short-circuit current (I_{sc}), MPP voltage (V_{mpp}), MPP current (I_{mpp}) and efficiency (η) [2]. These features are important to define the I-V curves of the PV panel in order to develop the MPPT controller unit. PV panel's I-V curves are a graphical representation of the relationship between the voltage and current of the solar panel for different temperatures and levels of irradiance [5]. Therefore, I-V curves provide all the necessary information required to perform the MPPT. Figure 1.1 shows the I-V curve for a given PV cell's temperature and solar irradiance. As it is well known, the power generated by a PV cell is the product of current and voltage at each point, hence, the P-V curve can be obtained and it is displayed in purple in Figure 1.1.

From the P-V curve, the maximum power generated by the solar panel (P_{max}) is obtained. This maximum power corresponds to the MPP and takes place for a specific combination of voltage (V_{mpp}) and current (I_{mpp}). Therefore, the ideal operating point of a PV panel corresponds to the MPP which varies according to the level of solar radiation and the temperature [2].

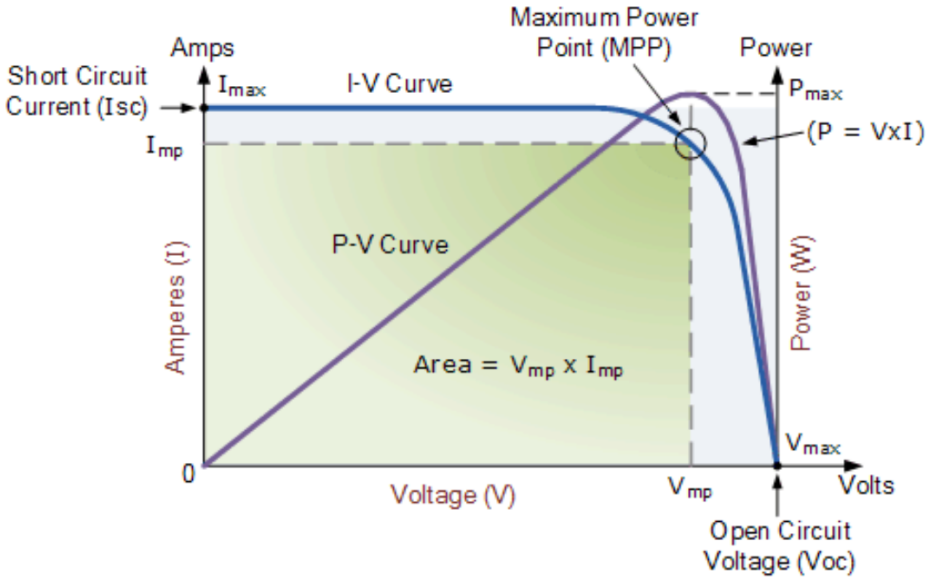

Figure 1.1: I-V characteristics of a generic solar panel [5].

There are different types of photovoltaic systems, however, the most common PV systems implemented nowadays are grid-connected [2]. This type of PV system is mainly composed of a solar array, a DC-DC converter with an MPPT controller unit and an inverter, as shown in Figure 1.2.

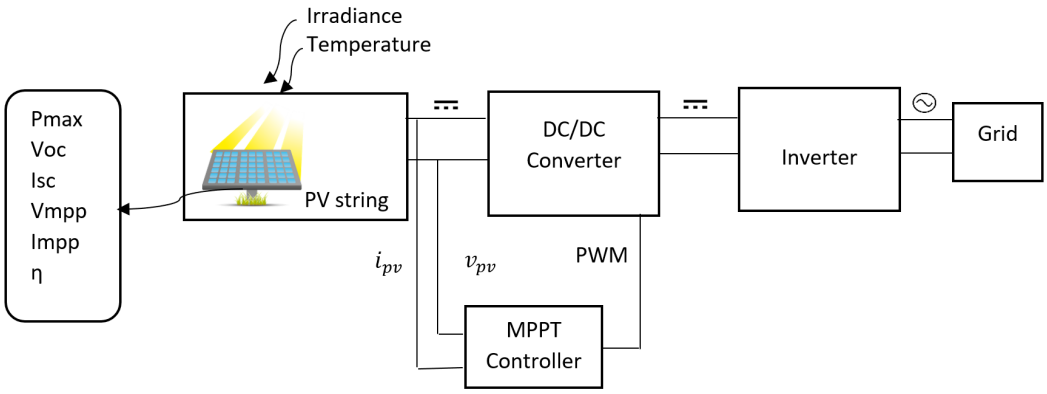

Figure 1.2: Basic block diagram of a PV system.

As mentioned at the begining of the chapter, PV modules can be connected to each other resulting in a PV array/string which generates electrical energy in the form of direct current. The MPPT controller unit takes the PV array's output voltage and current as input variables in order to calculate the ideal duty cycle.

This duty cycle is used to vary the Pulse Width Modulation (PWM) signal of the DC-DC converter in order to get the PV string to work continuously at its MPP. The output of the DC-DC converter is connected to an inverter to convert the DC electric energy in an AC electrical signal compatible with the grid.

1.2 MIC implementation

One of the most important factors to take into consideration when implementing PV modules is to constantly obtain the maximum energy possible out of these PV panels. If this is not done, the amount of energy that should have been obtained will instead be lost. Since energy is equal to power over time, power must be maximized when the energy is being extracted. To achieve such goal a MPPT needs to be implemented. This is an electrical system that is always on the search of the location of the MPP where the power generated by the PV module is maximum. MPPTs mostly consist of a power circuit that regulates either voltage drop or current flow across the PV terminals. There are different kinds of circuits that can be used to follow the MPP of the PV, this topic will be further introduced in chapter 3.

Solar plants and domestic installations are composed of several modules connected to each other in series or parallel configurations. To simplify the PV system's structure, one MPPT is commonly used for many modules as shown in figure 1.2. This approach may lead to unoptimal efficiency of the system since the uneven power generated by the PV modules might lead to have a system with a local MPP in addition to a global MPP [6]. In figure 1.3 a system exhibiting two MPP, due to partial shading, is shown. In order to ensure that the system is working in the global MPP and not in the local MPP, the controller will have to perform a voltage sweep in order to find the global MPP. This voltage sweep is a higher level of complexity in the MPPT control system [6]. In any case, the system will not be able to get the maximum power generation, as one panel is bypassed by a diode.

Another possible configuration is using MICs for each PV module which will result in higher overall efficiencies [8]. With this configuration, events like partial shading, uneven dirt, wear distribution or imperfections produced during the assembly line are reduced and do not affect the rest of the PV modules in the array. Also, a more detailed control of the plant is achieved since separate data from each individual panel is obtained [8]. As seen so far, different implementation options for MIC devices are possible but the most important objective of these devices is to individually control each PV module, resulting in an overall improved efficiency as well as a more robust system against any kind of disturbance [8]. Each PV module will then be connected directly to a MIC allowing the output voltage and current

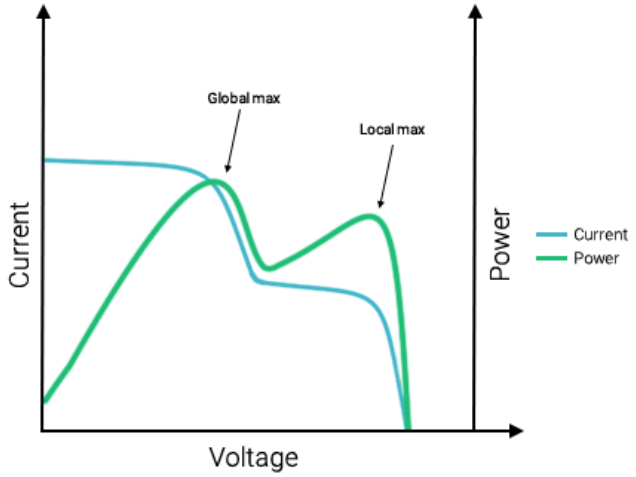

Figure 1.3: I-V curve of a system with more than one MPP [7].

to be defined by the load, either an inverter or a battery. This way the system is able to operate at different voltage and current levels whilst maintaining the MPP at all time [8].

MICs can be either microinverters or DC-DC converters. In figure 1.4 a PV system using MICs to perform the voltage reduction or increase is used. Notice that N panels might be used. Series or parallel connections can be used to link MICs' outputs and then connect this output to the inverter input through a DC link. The power rating of this inverter will have to be higher than the maximum power that can be delivered by MICs. Then the size of the inverter must consider the amount of PV panels installed.

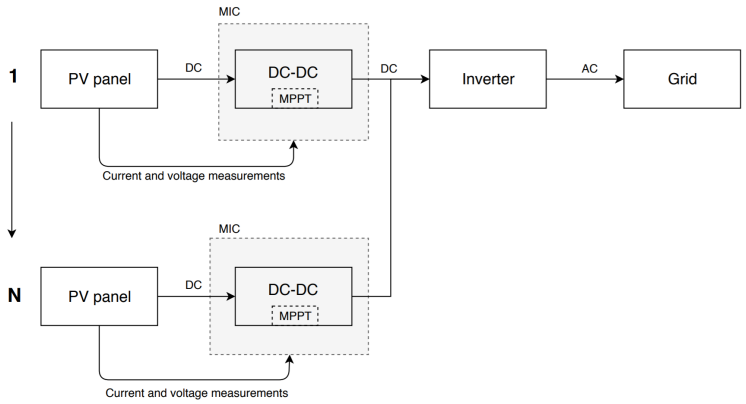

Figure 1.4: PV generation with DC-DC MIC system structure.

The panels with a MIC consisting on a microinverter, include a DC-DC converter with MPPT together with an inverter and are directly tied to grid. In figure 1.5 a microinverter system structure can be seen. For the user, this system is simpler, as only the PV must be purchased. The user doesn't have to worry about selecting and installing an inverter.

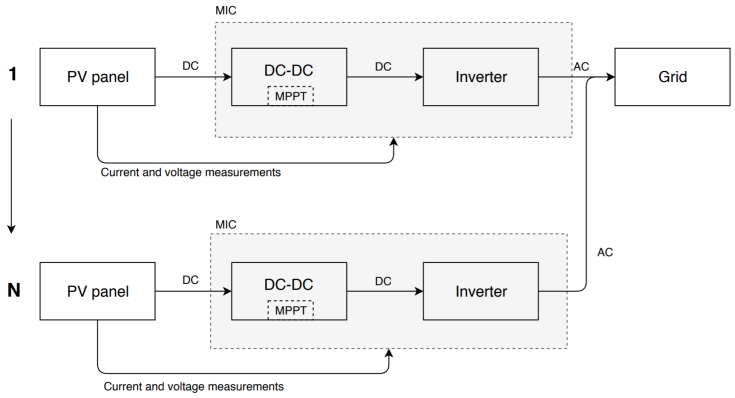

Figure 1.5: PV generation with microinverter MIC system structure.

The main advantage of the microinverter system is that it is simpler for the user, however, it implies an increase in costs and are usually less efficient than a DC-DC system with a higher power general inverter [8]. Therefore, for the development of this project a DC-DC MIC will be employed.

2 Problem Analysis

As discussed in chapter 1, uneven module power generation due to mismatches may lead to inefficient overall power generation. If one of the modules of the PV array is generating below average, it will affect the overall power generation. This situation can be addressed by placing a bypass diode in parallel with every PV panel as shown in figure 2.1. This way the current can flow through the diode, maintaining a higher current in the string [8]. However this solution will drive the power generation in the bypassed module to 0 and will cause a small power loss in the diode. Notice that the total power generated in the string is 120 W instead of 150 W.

For avoiding the loss of the power generated by the bypassed PV module, a MIC may be used [8]. These MICs are usually micro-inverters or DC-DC converters which incorporate a MPPT algorithm in order to maximize the power generated by the module. Microinverters are composed of a DC-DC converter with MPPT and an inverter to convert the DC current from the PV directly to AC current to be connected to the grid. DC-DC converters need an inverter at their output if the desired load is the grid. As the micro-inverters have reported higher cost and slightly lower efficiency [8] the project will be focused in developing a DC-DC MIC for integrating it with a single PV panel.

2.1 System requirements

For the design and test of the MIC it is of great importance to have the requirements of the system defined. The input requirements of the MIC will be based on the specifications of the PV panel *STP300S-20/Wfb* from Suntech Power. The specifications are shown in table 2.1.

The values from the previous table will be the input for the DC-DC converter.

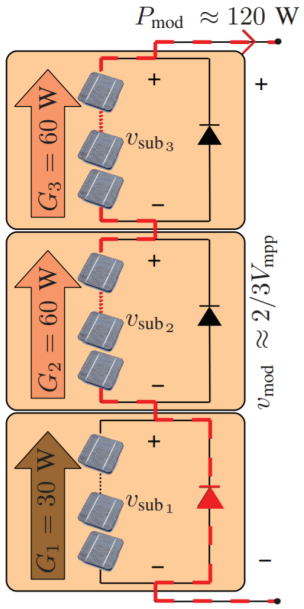

Figure 2.1: PV module being bypassed by a diode[8].

Maximum power (P_{max})	300 [W]
Optimum Operating Voltage (V_{mpp})	32.6 [V]
Optimum Operating Current (I_{mpp})	9.21 [A]
Open Circuit Voltage (V_{oc})	39.9 [V]
Short Circuit Current (I_{sc})	9.65 [A]
Module Efficiency (η)	18.3 %

Table 2.1: Electrical characteristics *STP300S-20/Wfb* [9].

The specifications of the load of the MIC will be based on the commercial inverter *"Power-one STGU-105"*[10] in order to have the output voltage defined. From the inverter's datasheet it is found that the nominal voltage in the DC-link is 360 V, with a maximum input power of 5500 W.
The development of this project will be based on these requirements because they are based on real commercial products that the user can purchase.

Table 2.2 shows the requirements of the MIC, extracted from the specifications of the PV panel and the inverter. It defines both the requirements regarding input, output and of the length of PV panel strings.

Input	
Maximum input power (P_{max})	300 [W]
Maximum input Voltage (V_{oc})	40 [V]
Maximum input current (I_{sc})	10 [A]
Minimum efficiency (η_{min})	98 %
Output	
Maximum output voltage (V_{out})	90 [V]
Maximum output current (I_{out})	15 [A]
Control	
Gain margin (GM)	To be defined
Phase margin (PM)	To be defined
Rise time (t_r)	To be defined
Overshoot (OS)	To be defined
PV system specification	
Minimum string length	4
Maximum string length	15
Others	
Maximum dimensions	To be defined
Operating Temperature	-40 to 85 [°C]

Table 2.2: MIC requirements.

2.2 Problem statement

The problem statement for this project can be formulated as the following question:

How can a module integrated converter be designed to maximize the PV power generation under real conditions?

The problem statement will be answered by fulfilling the following objectives:

- Design an efficient DC-DC converter for integration with a PV panel.
- Analyze different implementations of MPPT techniques and implement the selected control system.
- Hardware implementation of the MIC components including PCB layout.
- Test of the system using a PV simulator and validation of the results.

3 Background of converter topologies

3.1 Buck converter

A buck converter is one of the simplest DC-DC converters with the task of decreasing the input voltage. The required components are a DC-source for the input voltage, two switches (a diode and a transistor), an inductor, a capacitor and a load. The equivalent diagram in figure 3.1 illustrates a buck-converter.

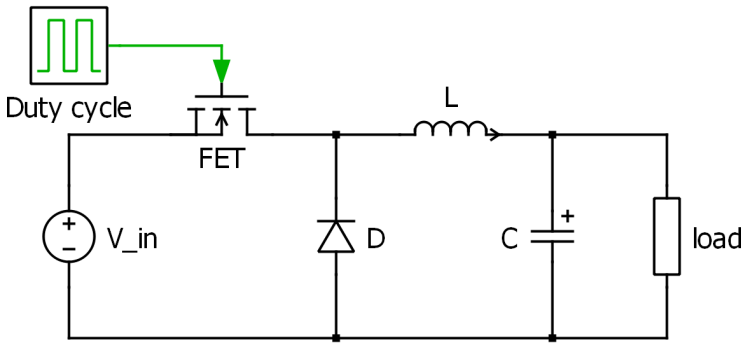

Figure 3.1: Buck-converter.

A buck-converter performs in two operating states. During the first state, the MOSFET is conducting and the diode is working as an open-circuit, the voltage drop then is divided between the inductor and load. Since the voltage is split, the voltage drop on the load is lower than the one of the input source. In addition, both the capacitor and the inductor are being charged. In the second state, the MOSFET

is switched off and the current flows through the diode. During this state, the inductor works as a current source and the capacitor stabilizes the voltage [11].

The main advantage for using the buck converter is that the structure is very simple and only one controlled switch is needed. Also, the component count and thus cost of components is low. Furthermore, the buck converter can reach efficiencies up to 99% [12].

However, this topology is not very versatile since it does not allow the increase of output voltage with respect to the input. Another drawback is the lack of galvanic isolation between the input and the output [13].

3.2 Boost converter

A boost converter is another type of DC-DC converter, it is similar to the buck but instead of lowering the output voltage, it produces a higher electrical potential at the output with respect to that at the input.

The circuit consists of two switches (a transistor and a diode), an inductor, a capacitor, a load and a DC-source for the input voltage. Figure 3.2 shows an equivalent circuit diagram with the aforementioned components.

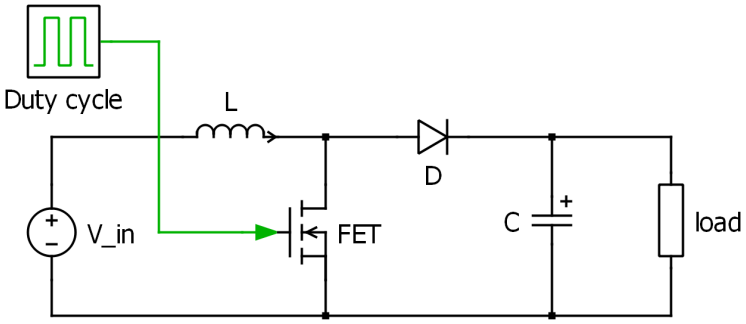

Figure 3.2: Boost-converter.

Similarly to the buck converter, this topology has two states, when the MOSFET is on, the current flows only trough the inductor because the diode is working as an open-circuit. Energy is then stored in the inductor, which voltage is equal to the input voltage, and current increases. Meanwhile, the capacitor releases the previously stored energy to the load. During the second state, the MOSFET is turned off, the current then loops trough the inductor, diode, capacitor and the load. Since the inductor had been previously charged, it now works as a current source in series with the voltage source of the circuit. The voltage across the load is then risen with respect to that at the input. Furthermore, the capacitor is charging [11].

An advantage for a boost converter is that it can raise the output voltage without using a transformer. It is also a cheap converter easy to control [14].

However, as it happened with the buck, the boost converter is also limited to rising the voltage and lowering it cannot be achieved. Also, if an error happens in the control of the MOSFET and it is left in ON-mode for a long time, a short-circuit is created and the current will increase until a component fails. Finally, this converter does not have galvanic isolation either.

3.3 Flyback converter

The flyback converter is another option for a DC-DC converter. It has galvanic isolation between the input and the outputs. The flyback converter is basically a buck-boost converter, but here the inductor is split to form a transformer. The windings of the transformer can have different turns ratio and in that way it is possible to step the voltage and current both up or down [15].

The basic circuit of the Flyback topology can be seen in figure 3.3. It consists of a DC-source, two switches (a transistor and a diode), two capacitors, a transformer and a load.

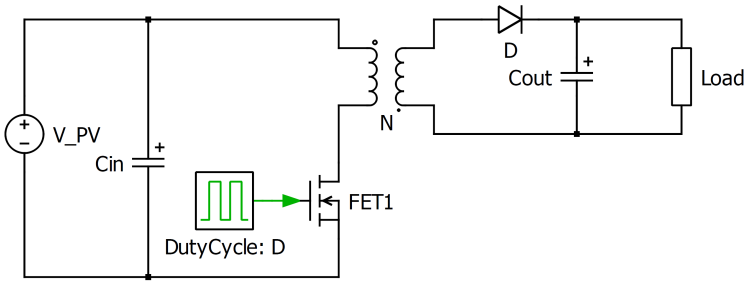

Figure 3.3: Flyback converter

When the MOSFET is on, the energy is transferred from the input voltage source to the transformer. In this state the output capacitor will supply the load with the output voltage. In the off-state the transformer will supply the output load with energy while it also charges the capacitor[15]. The transformer makes it possible to have multiple secondary windings, and therefore different output voltages. This can be used when designing the supply voltage for the control system[15].

The transformer makes it possible to have multiple secondary windings, and therefore output voltages. This can be used when designing the supply voltage for the control system[15].

The drawbacks are primarily the current and voltage waveforms. The voltage-drop across the two switches in their respective off periods, is decided by the input- and output voltages and the transfer ratio of the transformer. Furthermore

the leakage inductance from the transformer will result in a big voltage spike at the rising edge of the drain source voltage (V_{ds}) of the MOSFET. These needs to be reduced by a snubber circuit, like a RCD-circuit placed in parallel with the MOSFET[15]. This will increase the power loss and therefore decreasing the efficiency. The leakage inductance will also produce transients which will make the voltage stress at the MOSFET bigger and give high-frequency ringing at the input[16]. The V_{ds} is showed at figure 3.4 as V_{SW}.

Even though the transformer is be driven in continuous conduction mode (CCM), the currents in the windings will be discontinuous. This means that the RMS currents in both the primary and the secondary windings becomes higher[15]. The primary and secondary currents are shown at figure 3.4 as i_{pri} and i_{sec} respectively.

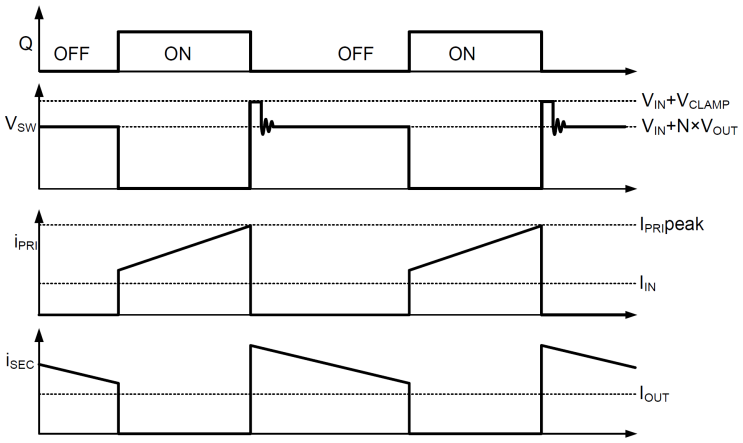

Figure 3.4: Flyback voltage and current waveforms[17]

3.4 Non-inverting buck-boost converter

The Non-inverting Buck-Boost converter is a DC to DC converter that allows the voltage at its output to be higher or lower than the voltage at its input. The topology can be seen in figure 3.5. It uses 4 switches, of which 2 are controlled devices.

The controller can force the system to work in any of the following modes:

1. Buck $\rightarrow D \subset [0,1]; D' = 0$
2. Boost $\rightarrow D = 1; D' \subset [0,1]$
3. Buck-Boost $\rightarrow D \subset [0,1]; D' \subset [0,1]$

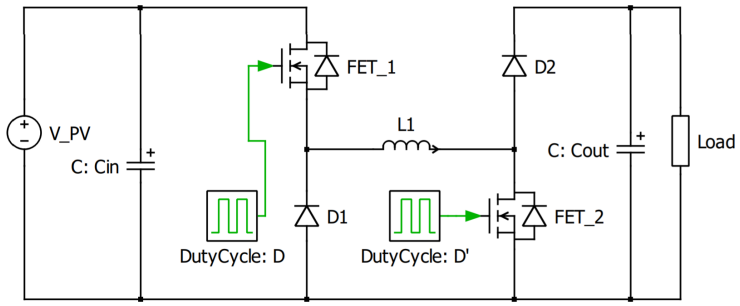

Figure 3.5: Non-inverting buck-boost converter.

Usually the inverter's input voltage is fixed to some value higher than the grid's voltage. The possibility of higher and lower voltages at the converter's output allows different ways of associating photovoltaic modules. Then the user is able to arbitrarily decide how many PV modules to link in series. Differently of what would happen in the case of Buck or Boost converters where the constraints regarding the number of panels are tighter.

Compared with other topologies that can have both higher and lower voltages at the output, such as the SEPIC converter, this DC-DC features a single inductor and no intermediate capacitor. See SEPIC schematic in figure 3.6, notice the additional inductor and capacitor. With such reduction in passive components the price, efficiency and power density improves significantly [16].

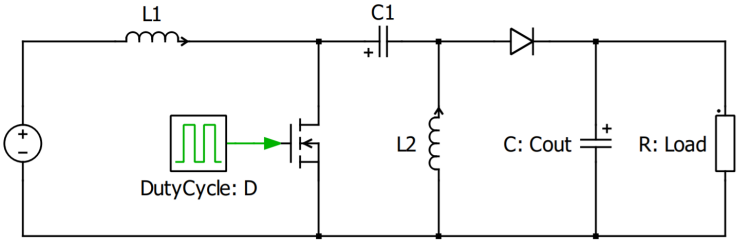

Figure 3.6: SEPIC converter.

One of the main drawbacks of the non-inverting buck-boost topology is the control's complexity, which must calculate the appropriate duty cycle D and D' in any of the modes and also the transition between these modes. The buck-boost mode is specially complicated as there are two duty cycles to calculate. This problem might be addressed by setting a constant duty cycle in one of the bridge's legs and then the control will calculate the other leg's duty cycle [18].

Although this topology exhibits appropriate features, it can be further improved by replacing the diodes by MOSFETs. The circuit may be seen in figure

3.8, it's called Bidirectional Non-Inverting Buck-Boost converter. With this variation, the following changes occur:

1. The system becomes bidirectional.
2. The conduction losses are smaller.

If the system is bidirectional it can be used in different MIC strategies, as the topology seen in figure 3.7, which features an isolated dc link. This topology needs a bidirectional MIC as energy flow in both directions is needed. It also allows diagnosis of PV modules, as described in section 3.5.

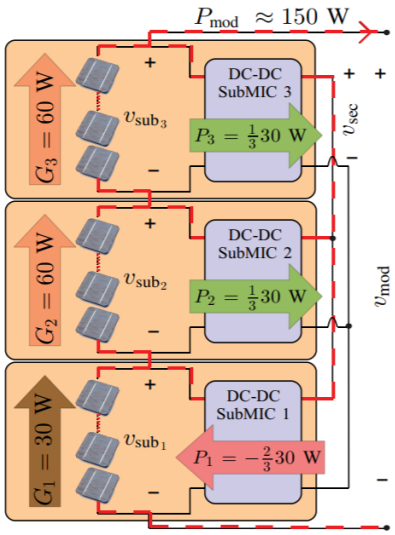

Figure 3.7: Bidirectional MIC use [8].

As seen in figure 3.8, notice that duty cycles of the switches that replace the diodes are $\overline{D}$ and $\overline{D'}$. This line over the variables means that it is the negated value of the original variable. The duty cycle is the boolean variable that indicates the conduction state of a switch. In the case of an enhancement switch, the switch is conducting whenever its driving duty cycle is equal to '1' and it is closed when its driving duty cycle is equal to '0'.

The main drawback is the increased difficulty of the driver circuitry and the requirement of a dead time in order to avoid the short circuit of FET_1 and FET_3 or FET_2 and FET_4, which could damage the system. When using diodes, the system is intrinsically protected against a shoot-through event.

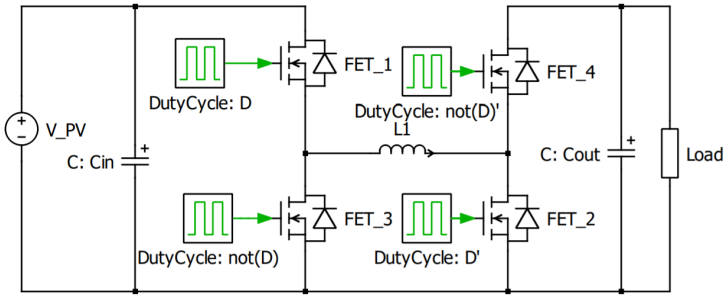

Figure 3.8: Bidirectional Non-inverting buck-boost converter.

3.5 Selection of topology

The selection of converter topology will be made based on the research made earlier in this chapter. The converter should be able to allow both a higher and a lower output than the input. This requirement will limit the buck and boost converters, which converts either up or down. This means that before the requirement is met, both a buck and boost converter must be a part of the implementation. This is not desirable, because it will introduce unnecessary work.

The next requirement states that the converter should have as high an efficiency as possible. The flyback converter will have a lower efficiency than the buck-boost, because of the transformer. This will introduce a loss in the extra inductor winding, and a larger loss in the FET because of the turns ratio in the transformer. Using a 4 transistor buck-boost converter, instead of a 2 transistor, it is possible to further optimizing the power loss because of the use of FET's instead of diodes.

The 4 transistor buck-boost converter does also have the advantage of being bidirectional. This means that it's possible to either extract current from the PV-module to the inverter at the output, or to inject current from the inverter to the PV-module. Due to that the PV-modules acts like LEDs, they will radiate an infrared light if current is injected. If the PV-modules are damaged in some way, i.e. having cracks, the radiation will be affected. This means that it is possible to discover faulty modules before efficiency drops. This will increase the overall efficiency of the system and ease the maintenance sequence significantly.

The Bidirectional Non-Inverting Buck-Boost converter is chosen because of these arguments. However the bidirectional functionality will not be addressed in this project, but could be a part of further development of the converter.

4 Non-inverting Buck-Boost converter design

4.1 Component sizing

4.1.1 Switch sizing

The system must regulate the power flow in order to maximize the power generation. In order to achieve this, the system includes switches that control the current flow. The switches consist on MOSFET devices. The switching frequency of the system is 50 kHz. Although the market has IGBT which can switch at 50 kHz, MOSFET devices allow lower losses than IGBTs for system's current rating. [19] [20]

The maximum output voltage of the system is 90V, however the voltage rating of the transistors was set to 150V in order to increase the reliability. The peak current through the transistors happens when the buck mode is activated. The peak current is equal to 14 A. In order to reduce the conduction losses and the heat sink size, a low on resistance is desired. This constraints were used when searching for the ideal component. The chosen device is the IPB200N15N3. It exhibits the features seen in table 4.1.

check with jesper if hhe did this calculation and then link, if not I calculated and have a photo of it

4.1.2 Heat sink sizing

The power dissipated in the switches is equal to the sum of the conduction losses and the switching losses. The conduction loss might be calculated as seen in equation 4.1.

$$P_{cond} = i(t)^2 \cdot R_{DS} \tag{4.1}$$

Maximum ratings	
Continuous I_D	40 [A]
V_{GS}	$\pm$ 20 [V]
Power dissipation	150 [W]
V_{DS}	150 [V]
R_{DSon}	20 [mΩ]
Other values of interest	
C_{GS}	1.81 [nF]
Package	D2PAK

Table 4.1: MOSFET figures of merit. T = 25 °C. [21]

The switching losses depend upon the switching frequency and the transistor's manufacturing characteristics. In order to calculate the value, the MOSFET's SPICE model was obtained from the manufacturer's website. The next step was to perform the simulation of the system. The system was simulated in both Buck and Boost modes. Special attention was put into the dead-band between PWM signals of different switches, to avoid current shoot through. After simulating, the average power dissipation under steady state was calculated in both Buck and Boost modes. Within every mode, the simulation was performed under the most unfavorable conditions, this is: Buck's output is 24 V and Boost's output is 90 V. The results can be seen in table 4.2.

R_{DS} is mainly dependant on the temperature. The models found neglect the temperature difference. Then, in order to get an approximated value considering temperature, the procedure will be to calculate the total losses at constant temperature using the SPICE model and then add the additional conduction losses due to the increase of the resistance, as expressed by equation 4.2.

$$\overline{P} = \overline{P_{loss,T=K}} + \overline{i(t)^2 \cdot \Delta R_{DS}} \tag{4.2}$$

Now the junction temperature based on the power dissipation calculated using the SPICE model is calculated. The case temperature is set to 50 °C, which is considered a realistic scenario. The thermal circuit can be seen in figure 4.1. The next step is to choose a commercial heat sink. The constraints are thermal resistance, size and price. TDEX6015/TH was found. Its features might be found in table 4.3. The switch temperature will be analysed in order to validate the heat sink.

$$T_J = T_{housing} + \overline{P_{loss,T=K}} + \cdot R_{thermal} \tag{4.3}$$

$$T_J = 50 + 5.54 \cdot 2.06 = 61.41^{\circ}\text{C} \tag{4.4}$$

Buck Mode	
M1	2.91 [W]
M2	0.82 [W]
M3	1.81 [W]
M4	0 [W]
Total	5.54 [W]
Boost Mode	
M1	0.69 [W]
M2	0 [W]
M3	0.48 [W]
M4	3.31 [W]
Total	4.48 [W]

Table 4.2: Average power dissipation in every MOSFET.

Features	
Size	60x60x16 [mm]
Thermal resistance	2 [K/W]

Table 4.3: Heat sink figures of merit.

The resistance is calculated as explained in equation 4.5. The resistance difference is relatively small.

$$\Delta R_{DS} = R_{DS,T=20°C} - R_{DS,T=61.41°C} = 4\ m\Omega \tag{4.5}$$

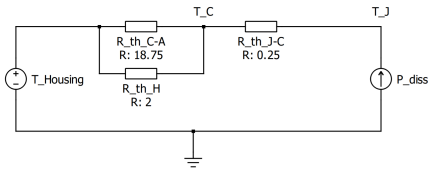

Figure 4.1: Thermal circuit used for sizing the heat sink

The full power dissipation values can be found on table 4.4. To achieve an exact result, the new total power should be used with the thermal circuit in order to calculate again ΔR_{DS}, but this difference is small and thus neglected. Now that the power dissipation has been calculated, the junction temperature must be checked in order to confirm that the heat sink has been properly sized. Equation 4.6 is used. The difference is fairly small and the junction temperature remains within safe area. Then TDEX6015/TH has been validated as a proper heat sink.

Switches power dissipation			
Switch	$\overline{P_{loss,T=K}}$ [W]	$\overline{i(t)^2 \cdot \Delta R_{DS}}$ [W]	**Total [W]**
Buck mode			
M1	2.91	0.39	**3.30**
M2	0.82	0.21	**1.03**
M3	1.81	0.58	**2.39**
M4	0	0	**0**
Total	5.54	1.18	**6.72**
Boost mode			
M1	0.69	0.28	**0.97**
M2	0	0	**0**
M3	0.48	0.12	**0.6**
M4	3.31	0.18	**3.49**
Total	4.48	0.58	**5.06**

Table 4.4: Table dissipation including the extra dissipation due to the increase of temperature.

$$T_J = 50 + 6.72 \cdot 2.06 = 63.84^{\circ}\text{C} \tag{4.6}$$

4.1.3 Driver circuitry

*why driver circuitry *different driver grounds –> solution, no bootstrap *gate pull down resistor *gate resistor sizing, effect over switching frequency *calculated/simulated switching losses *layout considerations

4.2 Sensors

To implement the MPPT it's necessary to measure the output voltage and current of the PV-module. These measurements will be obtained by implementing a voltage and current sensor. A second voltage sensor will be implemented to measure the output voltage of the DC/DC coverter, for possible future use.

To protect the RT-Box, it has been chosen to fully isolate it from the power stage of the converter. To do so, the sensors will have to include isolation between input and output.

4.2.1 Input voltage sensor

The voltage sensor selected is ACPL-C870. This sensor includes a optical isolation amplifier, which makes it well suited for isolated voltage sensing. Some relevante

electrical specifications have been included in table 4.5. Figure 4.2 shows the placement of the two voltage sensors, where V_{in} and V_{out} are the input and output sensor respectively.

Recommended ratings		
Supply voltages	V_{DD1}, V_{DD2}	5 [V]
Input voltage range	V_{in}	$0 - 2$ [V]
Other values of interest		
Voltage gain	G	1 [V/V]
Output common-mode voltage	V_{OCM}	1.23 [V]
Gain tolerance	–	± 3 [%]
Bandwith	BW	100 [kHz]
Package	SSOP	[-]

Table 4.5: Electrical specifications ACPL-C870 [22]

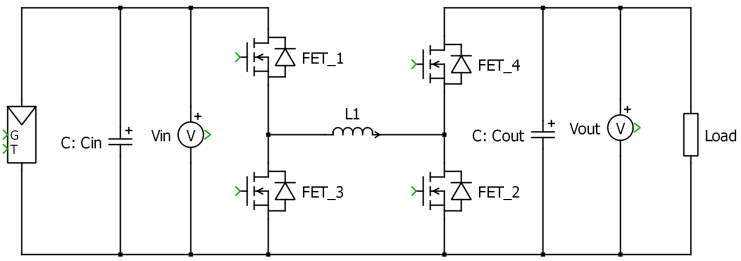

Figure 4.2: Voltage sensors placement

Voltage divider

The input voltage at the voltage sensor is recommended to be in the range of $0V - 2V$. To divide the measured voltage into that range, a voltage divider will be implemented.

The maximum output voltage of the PV-module is the open-circuit voltage at $45.2V$. To achieve a safety margin and to make the converter adaptable to other types of PV-modules, $50V$ has been selected. The current flow in the voltage divider has been set at $1mA$, to secure a insignificant power loss. The resistors can be calculated with the following equations:

$$R_{17} = \frac{V_{in,max} - V_{out}}{I} = \frac{50V - 2V}{1mA} = 48k\Omega \tag{4.7}$$

$$V_{out} = V_{in,max} \cdot \frac{R_{18}}{R_{17} + R_{18}} \Rightarrow 2V = 50V \cdot \frac{R_{18}}{48k\Omega + R_{18}} \tag{4.8}$$

$$R_{18} = 1.958k\Omega$$

To achieve these resistor values $R_{17} = 47k\Omega$ and $R_{18} = 2k\Omega$ have been chosen.

Filtering

For a stable MPPT control, the measured voltage must have a very low ripple. To ensure this, a low-pass RC filter with a corner frequency at $500Hz$, will be placed between the voltage divider and the sensor. The resistor of the filter will be R_{17} in the voltage divider. The capacitor will calculated as followed in equation 4.9:

$$C_{17} = \frac{1}{2\pi \cdot f_c \cdot R_{17}} = \frac{1}{2\pi \cdot 500Hz \cdot 47k\Omega} = 6.7nF \tag{4.9}$$

To achieve the capacitance $C_{17} = 6.6nF$ has been chosen.

Amplification

The input range of the ADC in the RT-Box is $0V - 5V$. To take advantage of the full range an amplifier will be implemented. The output of the voltage sensor is differential with an offset at $1.23V$. Therefore a differential amplifier will be implemented using a LMC6484 quad operational amplifier. By using a quad amplifier, the same IC can be used for all the sensors. The relevant electrical specifications have been included in table 4.6

Recommended ratings		
Supply voltage	V_{DD}	$3 - 15.5$ [V]
Input voltage range	V_{in}	$\pm V_{DD}$ [V]
Other values of interest		
Slew rate	SR	1.3 $[V/\mu s]$
Gain-Bandwith product	GBW	1.5 $[MHz]$
Number of amplifiers	–	4 [-]
Package	–	SOIC [-]

Table 4.6: Electrical specifications LMC6484 [23]

The resistors of the differential amplifier will be sized with equation 4.10.

$$V_{out} = \frac{R_{22}}{R_{20}} \cdot (V_2 - V_1) \tag{4.10}$$

Where $V_2 - V_1$ is the difference between the output pins of the voltage sensor. With unity gain in the voltage sensor, the maximum difference at the output will be $2V$. This should correspond to the maximum input voltage of the ADC at $5V$. R_1 is selected to be $11k\Omega$. The resistor R_{22} is now calculated using equation 4.10.

$$5V = \frac{R_{22}}{11k\Omega} \cdot 2V \tag{4.11}$$

$$R_{22} = 27.5k\Omega$$

To achieve the value of R_{22} it's rounded to be $27k\Omega$. Furthermore $R_{19} = R_{20}$ and $R_{21} = R_{22}$, to get a balanced differential amplifier.

The circuit

The circuit regarding the input voltage measurement is shown at figure 4.3. V_{in} is the measured voltage from the PV-module. The points $OA1_+$ and $OA1_-$ are connected to the non-inverting and inverting input of the amplifier respectively. $OA1_{out}$ is connected to the output of the amplifier. C_{15} and C_{16} are decoupling capacitors for the two supply voltages. The maximum input voltage of the voltage sensor is $5V$. Because of this a $4.7V$ zener diode has been added at the input, to protect it from over-voltage.

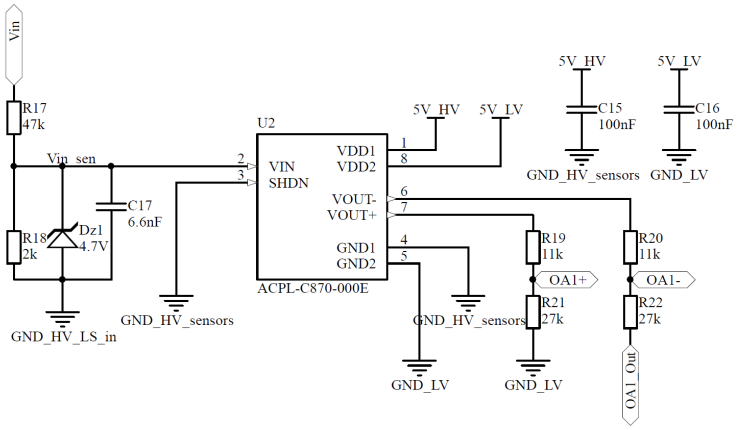

Figure 4.3: Input voltage sensor

4.2.2 Output voltage sensor

The voltage sensor at the output is design by the same procedure as the input sensor. The voltage divider will designed such that the values of the amplifier can be reused.

Voltage divider

The maximum output voltage of the DC/DC converter will be $90V$, when only 4 PV-modules are used. To insert a safety margin if one converter fails, the maximum sensed voltage will be designed at $120V$.

The resistors will be sized by reusing equation 4.7 and 4.8.

$$R_{26} = \frac{V_{in,max} - V_{out}}{I} = \frac{120V - 2V}{1mA} = 118k\Omega \tag{4.12}$$

$$V_{out} = V_{in,max} \cdot \frac{R_{27}}{R_{26} + R_{27}} \Rightarrow 2V = 120V \cdot \frac{R_{27}}{118k\Omega + R_{27}} \tag{4.13}$$
$$R_{27} = 2.03k\Omega$$

To achieve these resistor values $R_{26} = 120k\Omega$ and $R_{27} = 2k\Omega$ have been chosen.

Filtering

The filter will be design with the same corner frequency at $500Hz$, as for the input sensor.

The resistor of the filter will be R_{26} in the voltage divider. The capacitor will be calculated as followed in equation 4.14:

$$C_{22} = \frac{1}{2\pi \cdot f_c \cdot R_{26}} = \frac{1}{2\pi \cdot 500Hz \cdot 120k\Omega} = 2.7nF \tag{4.14}$$

To achieve the capacitance $C_{22} = 3.3nF$ has been chosen. By using these values the actual corner frequency will be $402Hz$.

The circuit

The circuit regarding the input voltage measurement is shown at figure 4.4.

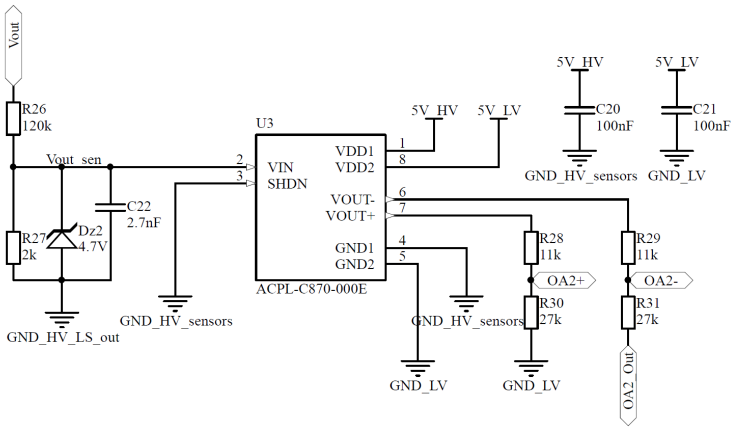

Figure 4.4: Output voltage sensor

4.2.3 Current sensor

The current along with the voltage of the PV allows the system to perform power calculation, which is needed for the MPPT algorithm. The current will be measured in parallel with the inductor with a hall effect sensor. Placing it in series with the

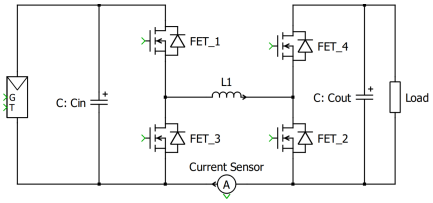

Figure 4.5: Current sensor placement.

PV module would be the easiest approach for MPPT, but placing it in parallel with the inductor allows implementing a current controller for possible future use.

The sensor is a ACS723-20AB which is a Hall effect sensor. Its features might be found in table 4.7.

Maximum ratings	
Supply voltage	4.5-5.5 [V]
Gain	100 [mV/A]
Input range	±20 [A]
Other values of interest	
Bandwidth	20 or 80 [kHz]
Package	SOIC8

Table 4.7: Current sensor figures of merit. [**current_sensor**]

The output of the sensor is a voltage proportional to the current following the next equation:

maybe the gain is 0.125, to be confirmed by test.

$$V_{current} = \frac{1}{10}\, i + 2.5 \tag{4.15}$$

In order to ease the task of the control, the signals are filtered by hardware. The current will be used by the MPPT, which frequency is $100Hz$. The sensor output is filtered by a LPF which cut-off frequency is $500Hz$. The cut-off frequency has been calculated by a hundredth of the switching frequency, which is $50kHz$. Also the current might be used in the current controller, this signal will be filtered at $80KHz$ in order to remove high frequency noise, this cut-off frequency was selected as it is the sensor's bandwidth. The filters are first order low-pass filters implemented with a resistor in series with a capacitor.

check final implementation

has the current control been implemented? was enough this filtering?

In order to calculate the current from the PV module, the converter working mode will have to be taken into account. Assuming continuous conduction mode, the average PV current is:

$$Buck\ mode \rightarrow \overline{I_{in}} = i_{measured} \cdot \delta \tag{4.16}$$

$$Boost\ mode \rightarrow \overline{I_{in}} = i_{measured} \cdot \tag{4.17}$$

$$Buck - Boost\ mode \rightarrow \overline{I_{in}} = i_{measured} \cdot \delta \tag{4.18}$$

The IC has been placed far from the inductor in order to avoid undesired magnetic flux.

4.3 Power Supplies

In the first iteration of the converter, the drivers and the sensors will be supplied by an external $12V$ voltage source. This source will be used directly to supply the two lower leg MOSFET drivers. To support the higher leg drivers, two isolating $12V$ supplies will be used, with the external $12V$ as input. These will be two TRACO supplies *TMA1212S* [24]. The chosen voltage sensors need a $5V$ power supply at both input and output of the sensor. These should isolated from each other. The input side will be supplied by a $5V$ voltage regulator, *LD1117* [25], and the output side will be supplied by the RT-box. The current sensor will also be supplied with $5V$ by the RT-box. A LED will be added to every voltage source, to indicate if they are on.

5 Maximum Power Point Tracking

5.1 Evaluation of main MPPT techniques

5.1.1 Constant voltage algorithm

Empirical experiments have shown that the voltage has a linear dependence on the MPP at different ambient conditions. The MPP is in the range of 70 to 80 of the open circuit voltage. The advantage of this algorithm is that only the voltage is measured and the control of the system is done by a simple control loop. The location of such PV-panels with the constant voltage as MPP algorithm is only possible in regions with low temperature fluctuations. The reason for this disadvantage is that with strong temperature fluctuations the point of the MPP varies very strongly and the assumption of linear dependence is no longer valid. In addition, it does not work with PV panels which are partially shaded.[]

5.1.2 Perturb and Observe

Perturb and observe is with the incremental conductance the most frequently used algorithm for MPPT. With perturb and observe, the currently measured power is periodically compared with the previous power. If the measured power is greater than the power from the previous measurement, the voltage is further increased to reach the MPP. If a power reduction is detected after the comparison, the voltage is reduced. The flowchart in the figure 5.1 illustrates this method. The classical algorithm uses a fixed step to change the voltage. When the MPP is reached, the algorithm oscillates around the MPP. If the fixed step value is high, the MPP is reached quickly. On the other hand, the oscillation around the MPP is high, which reduces the efficiency. The advantage of a small value is that the oscillation is smaller, but it takes more time to reach the MPP.

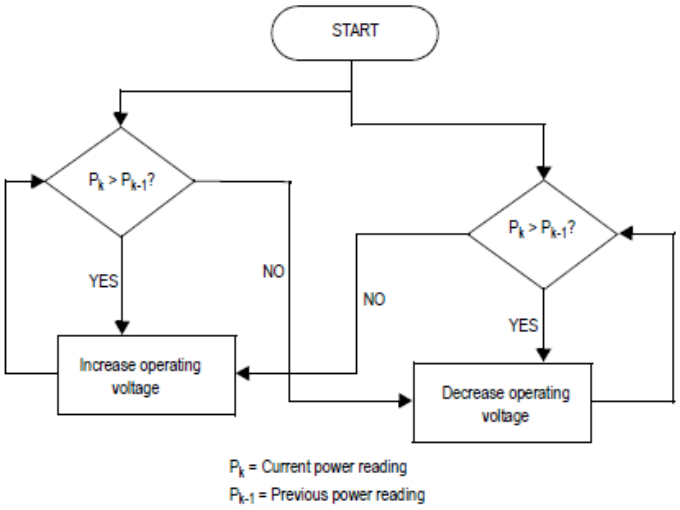

Figure 5.1: flow chart from perturb and observe.picture should change

5.1.3 Incremental conductancee

The approach of incremental conductance is that the MPP is at the position where the derivative of power after voltage is 0. The left side of the MPP is the derivative greater than 0 and the right side is the derivative less than 0, which is what the equations describe. The algorithm compares the incremental conductance with the previous one to then increase (left side of the MPP) or decrease (left side of the MPP) the voltage. In this procedure, the algorithm is stopped when the MPP is reached. There is no oscillation around the MPP. If a change in current is detected, the algorithm starts to find the MPP again, as you can see in the flowchart in figure **??**. As with perturb and observe, a fixed value is used to change the voltage. If the value is high, the probability is higher that the algorithm oscillates around the MPP.

5.2 Selection of MPPT algorithm

5.3 Implementation of Perturb and Observe algorithm

Things to write in this section:

- Why we use duty cycle as output of the MPPT instead of a voltage ref.
- Frequency of the MPPT algorithm is 100Hz. Every 10ms the MPPT evaluates voltage and power to decide if it is necessary to increase or decrease D.

- Initial conditions: enable the MPPT after 5Ts (50ms) to ensure that Vin has reached the open circuit voltage, counter = 5 to have some open loop measurements before starting the voltage evaluation, the system starts in buck mode (D=0.25) with fix variations of duty cycle (0.01), limits of duty cycle 0.05<D<0.95 to avoid problems in buck and in boost mode respetively.

- The current measurement is carried out in the inductor instead of in the panel so it is possible to implement future PI control loops to improve the MPPT algorithm. For this reason it's necessary to make a transformation of this current in the case of buck mode (multiplying by the corresponding duty cycle, Dbuck = 2*D). However in boost mode it's not necessary because the panel current is the same as the inductor's current.

- Mode decision is done by mapping the transfer functions (refer to Figures) corresponding to buck and boost mode and including an extra block after the MPPT which has as input the value of D and returns the duty cycle for buck or boost mode. This duty cycles are used to generate the corresponding PWM signals according to the mode the converter is working at each time.

- Also mention the case when a change in irradiance takes place it's a good idea to reset the value of delta D to 0.01. This is because we are using variable step and when the system detects the change in irradiance it will keep the corresponding value of delta D which will be very small because the system already could have reached the MPP (variable step).

- The MPPT algorithm is an improved version of the simple one explained in the previous section as it reduces the duty cycle step/increment by 2 iteractively when it detects it has reached the MPP.

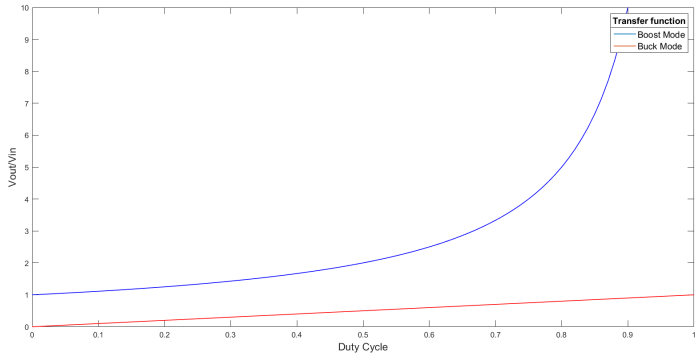

Figure 5.2: Transfer function of buck mode and boost mode.

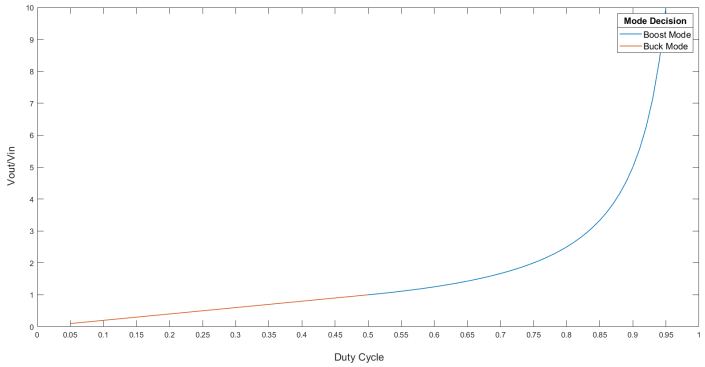

Figure 5.3: Mapping to decide the mode of operation.

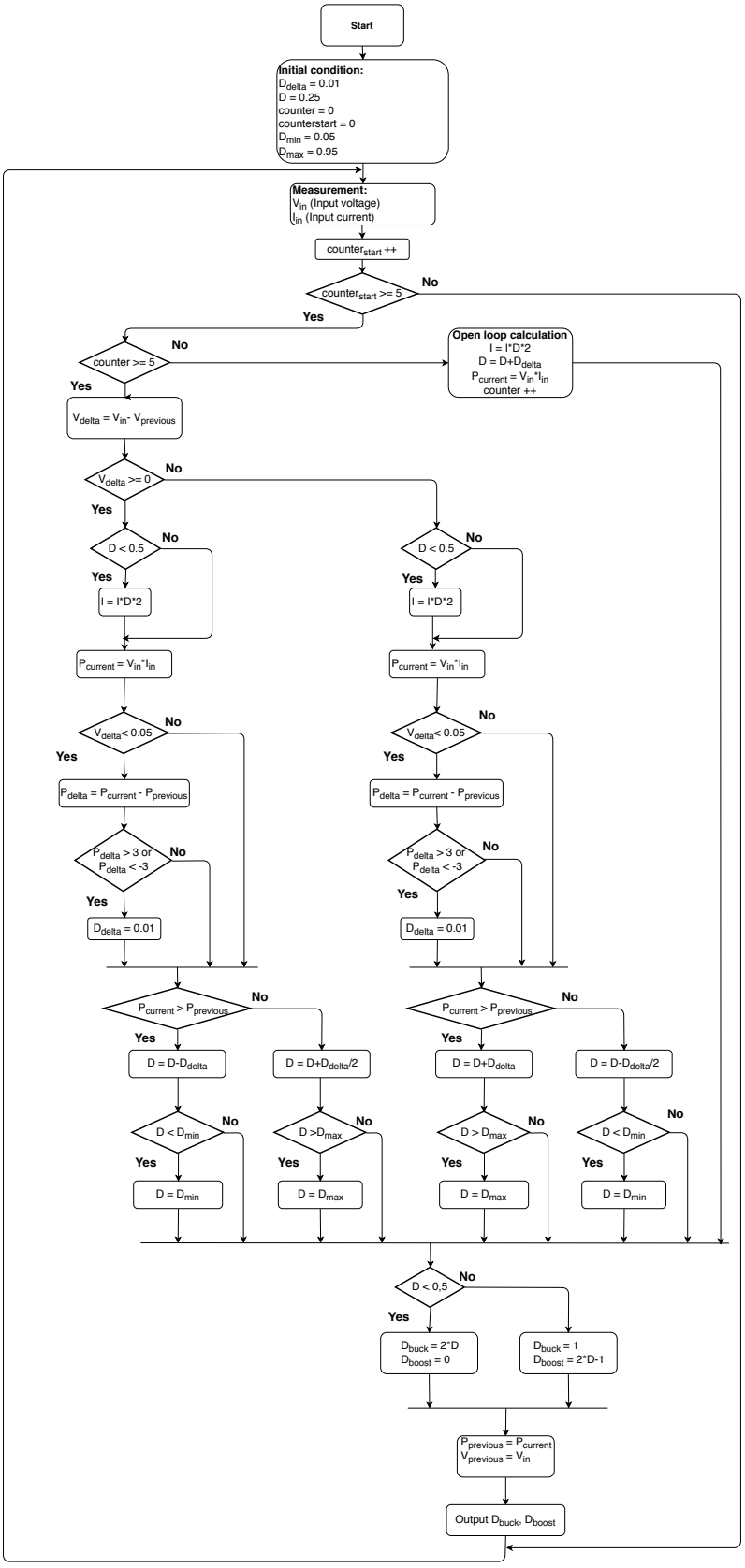

Figure 5.4: flow chart final

5.4 Simulation of the MPPT algorithm

5.4.1 Model of the PV panel

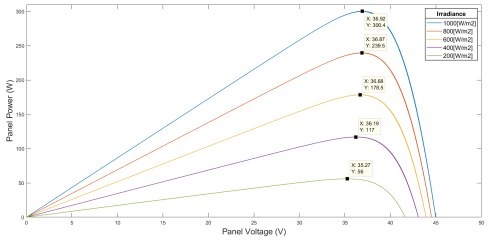

Figure 5.5: PV curves for constant T(25deg) and change in I.

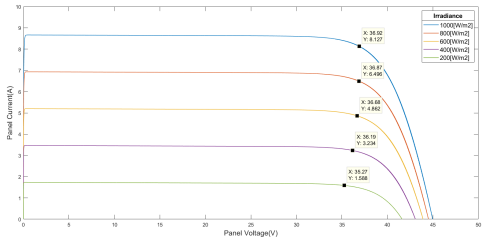

Figure 5.6: IV curves for constant T and change in I.

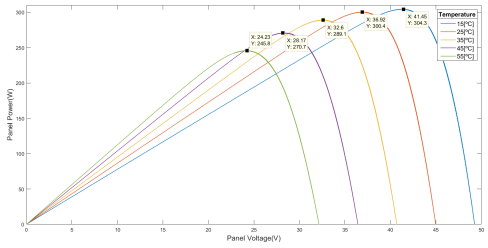

Figure 5.7: PV curves for constant I(1000) and change in T.

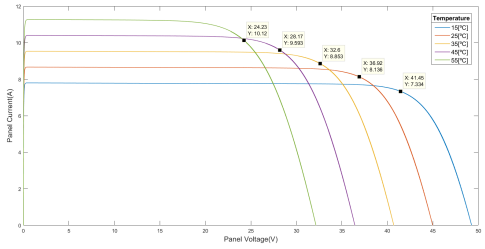

Figure 5.8: IV curves for constant I(1000) and change in T.

5.4.2 MPPT algorithm results

Bibliography

[1] UN Environment. *Renewables 2018 - Global Status Report*. Sept. 25, 2018.

[2] Michael Boxwell. *Solar Electricity Handbook - A simple, practical guide to solar energy-designing and installing solar PV systems*. 2017.

[3] Binod Prasad Koirala, Benjamin Sahan, and Norbert Henze. *Study on MPP mismatch losses in photovoltaic applications.* Sept. 25, 2014.

[4] *Photovoltaic effect*. Apr. 13, 2017. URL: https://solar-energy.technology/definitions/photovoltaic-effect.html.

[5] *Solar Cell I-V Characteristics*. Oct. 4, 2018. URL: http://www.alternative-energy-tutorials.com/energy-articles/solar-cell-i-v-characteristic.html.

[6] Microchip. *Practical Guide to Implementing Solar Panel MPPT Algorithms, AN1521*. 2013.

[7] *Know how inverter MPPT functionality affects performance*. Mar. 7, 2018. URL: https://www.solarpowerworldonline.com/2018/03/install-tip-inverter-mppt-functionality-affects-performance/.

[8] Carlos Olalla, Daniel Clement, and Miguel Rodriquez. *Architectures and Control of Submodule Integrated DC–DC Converters for Photovoltaic Applications*. June 6, 2013.

[9] Suntech Power. *PV-modul 290-300W (Suntech-power).pdf*. 2018.

[10] Power-One. *Power-one Inverter.pdf*. 2018.

[11] Minh Quan Duong, Hien Tran, and Chowdhury Akram Hossain. *Influence of Elemental Parameter in the Boost And the Buck Converter*. Dec. 21, 2017.

[12] ROHM Semiconductor. *Efficiency of buck converter*. Dec. 2016.

[13] *Buck Converter Tutorial*. Sept. 27, 2018. URL: http://www.completepowerelectronics.com/buck-converter-tutorial-topology-working-advantages-applications/.

[14] *Boost Regulator Tutorial: Topology Working*. Sept. 27, 2018. URL: http://www.completepowerelectronics.com/boost-regulator-tutorial-topology-working-advantages-applications/.

[15] R. Kanthimathi and J. Kamala. *Analysis of different Flyback Converter Topologies*. May 30, 2015.

[16] Texas Instruments. *Under the hood of a noninverting buck-boost converter*. Sept. 1, 2016.

[17] Texas Instruments. *Isolated Continuous Conduction Mode Flyback Using the TPS55340*. Jan. 2013.

[18] STMicroelectronics. *Buck-boost converter using the STM32F334 Discovery kit, AN4449*. Sept. 2014.

[19] *Lecture 7: MOSFET, IGBT, and Switching Loss*. Nov. 13, 2018. URL: http://web.eecs.utk.edu/~dcostine/ECE481/fall2013/lectures/L7_slides.pdf.

[20] *IGBT or MOSFET: Choose Wisely*. Nov. 13, 2018. URL: https://www.infineon.com/dgdl/Infineon-IGBT_or_MOSFET_Choose_Wisely-ART-v01_00-EN.pdf?fileId=5546d462533600a40153574048b73edc.

[21] *IPB200N15N3GATMA1 Datasheet*. Apr. 28, 2010. URL: https://docs-emea.rs-online.com/webdocs/1090/0900766b810908e8.pdf.

[22] Avago Technologies. *ACPL-C87B, ACPL-C87A, ACPL-C870*. Mar. 4, 2013. URL: https://docs-emea.rs-online.com/webdocs/116c/0900766b8116c0f3.pdf (visited on 11/16/2018).

[23] Texas Instruments. *LMC6484 CMOS Quad Rail-to-Rail Input and Output Operational Amplifier*. Sept. 2015. URL: http://www.ti.com/lit/ds/symlink/lmc6484.pdf?fbclid=IwAR2-z4SAec11ZMHQGk9z1CUVKjUphWbEPVIUkoxwhvqeh_Ap6lwYe6sYFbk (visited on 11/16/2018).

[24] Traco Power. *DC/DC Converters - TMA series, 1 Watt*. Feb. 11, 2014. URL: https://docs-emea.rs-online.com/webdocs/153a/0900766b8153aa01.pdf (visited on 11/16/2018).

[25] ST Microelectronics. *LD1117xx*. July 2009. URL: https://docs-emea.rs-online.com/webdocs/0dbd/0900766b80dbda35.pdf (visited on 11/16/2018).

A

Buck-boost equations

The way the buck-boost converter works has been discussed in the introductory chapter .... The equations that can be used for this type of converter depends on, in which mode the converter are working in. When working in the buck mode the equations below will be used when we see the converter as ideal.

A.1 Buck mode

The voltages and currents in the different switch stages can be seen in figure A.1

Working in CCM mode means that the current through the inductor never falls to zero. When the switch is on(closed) the voltage across the inductor will be:

$$V_L = V_i - V_o \tag{A.1}$$

The current through the inductor rises linearly and no current will flow through the diode. When the switch is off(open) the diode will be forward biased which means the voltage across the inductor will be:

$$V_L = -V_o \tag{A.2}$$

As seen in the figure A.1 the current will decrease in this state but never to reaches zero.

This equations shows that energy will be stores in the inductor during the on time and decreases in the off time. This means that the inductor is used to transfer the energy from the input to the output of the converter. Looking at the voltage part of the figure the yellow surface corresponds to $(V_i - V_o) * t_{on}$ and the orange correndsponds to the $-V_o * t_{on}$. When working in a steady state operation these areas must be equal which in reduced form will be:

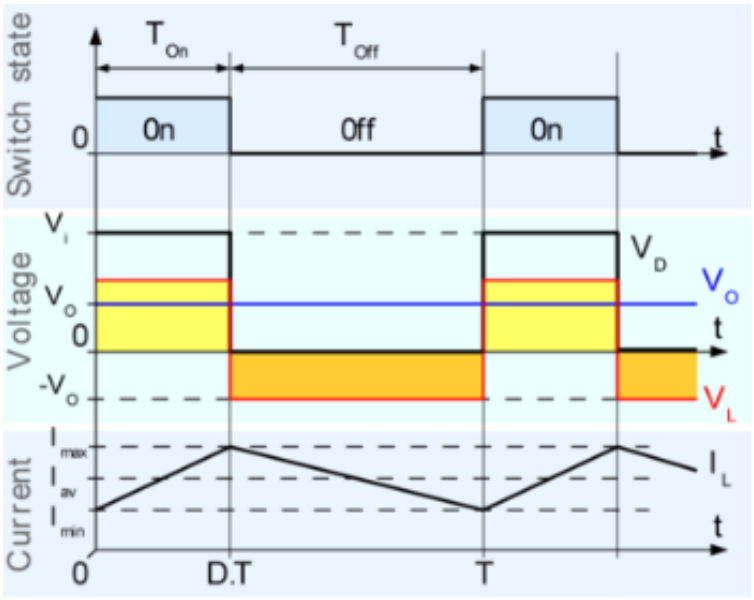

Figure A.1: Ideal buck converter in CCM picture ref

$$V_o = D * V_i \tag{A.3}$$

Where $t_{on} = D * T$ and $t_{off} = (1 - D) * T$. It can be seen that the output voltage will vary linearly with the duty cycle for a given input voltage.

The current seen at the output will be the average current from both modes:

$$I_{Lavg} = I_o \tag{A.4}$$

The ripple current in the inductor can be found with the frequency and inductance:

$$\Delta I_L = \frac{V_i * D(1 - D}{L * f} \tag{A.5}$$

The maximum current ripple through the inductor can be found by looking at the maximum input voltage:

$$\Delta I_{Lmax} = \frac{(V_{imax} - V_o) * D}{L * f} \tag{A.6}$$

That equation will be used to calculate the peak current in the inductor:

$$I_{Lmax} = I_o + \frac{\Delta I_{Lmax}}{2} \tag{A.7}$$

There are several factors that contribute to the output voltage ripple. Basically the output voltage will rise and fall when the capacitor is charging and discharging. It can be found by calculating $\Delta V_o = \frac{\Delta Q}{C}$, where ΔQ is the amount of charge. This value is found by integrating I_L from t_1 to t_2. By doing that $\Delta Q = \frac{\Delta I_L}{8} * T_s$. Which means the output voltage ripple can be calculated with:

$$\Delta V_o = \frac{\Delta I_L}{8 * C * f} \tag{A.8}$$

A.2 Boost mode

When working in boost mode the output voltage will be larger than the input voltage. The voltages and currents in the different switch stages can be seen in figure A.2

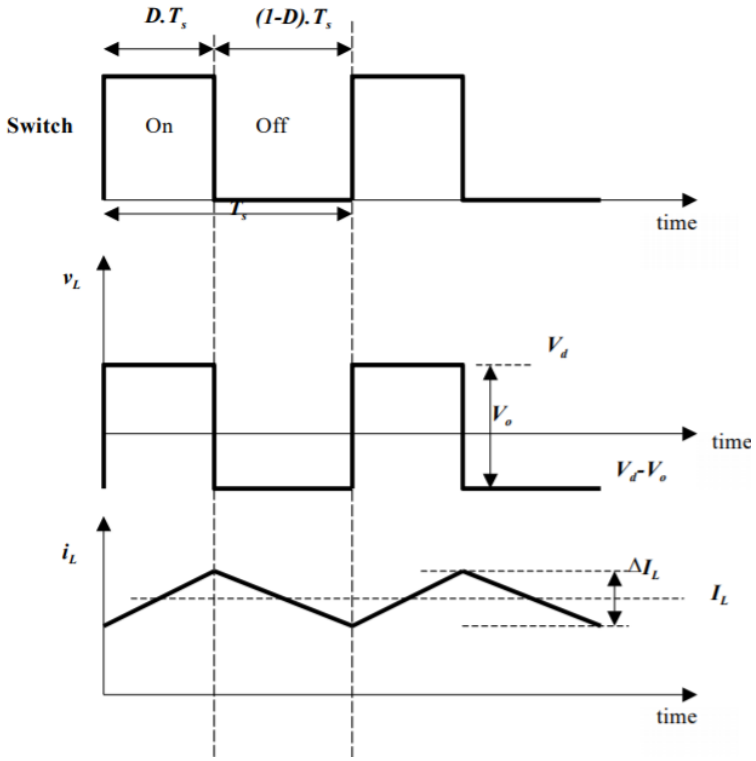

Figure A.2: Ideal boost converter in CCM picture ref

In the boost mode CCM will still be used. When the switch is on the voltage across the inductor will be:

$$V_L = V_i \tag{A.9}$$

In this state the inductor current will increase. On the other hand in the off-state the inductor will transfer its energy to the capacitor. Here the voltage across the inductor will be:

$$V_L = V_i - V_o \tag{A.10}$$

In figure A.2 it can be seen that we are working in CCM because the current never reaches zero. When working in steady state the increase of energy stored in the inductor must be equal to the energy transferred to the capacitor during the off state. This means that $\Delta I_{Lon} + \Delta I_{Loff}$. Integrating and reducing these expressions will lead to:

$$V_o = \frac{1}{1-D} * V_i \tag{A.11}$$

The average current through the inductor will be calculated as below:

$$I_{Lavg} = \frac{1}{1-D} * I_o \tag{A.12}$$

The ripple current through the inductor can be found using the frequency and the inductance:

$$\Delta I_L = \frac{V_i * D}{L * f} \tag{A.13}$$

The maximum ripple current through the inductor will be found with the maximum input voltage:

$$\Delta I_{Lmax} = \frac{V_{imax} * D}{L * f} \tag{A.14}$$

With the above equation the peak current through the inductor can be found like this:

$$I_{Lmax} = \frac{1}{1-D} * Io + \frac{\Delta I_{Lmax}}{2} \tag{A.15}$$

The output voltage ripple can be found by calculating $\Delta V_o = \frac{\Delta Q}{C}$, where ΔQ is the amount of charge. This value is found by integrating $\frac{-I_o}{c}$ from D to 0. By doing that the output voltage ripple can be calculated with:

$$\Delta V_o = \frac{D * I_o}{f * c} \tag{A.16}$$